Applied Soft Computing Journal 83 (2019) 105620

Contents lists available at ScienceDirect

Applied Soft Computing Journal

journal homepage: www.elsevier.com/locate/asoc

Short-term passenger flow prediction under passenger flow control using a dynamic radial basis function network

Haiying Li [a], Yitang Wang [a], Xinyue Xu [a,*], Lingqiao Qin [b], Hanyu Zhang [a]

[a] State Key Laboratory of Rail Traffic Control and Safety, Beijing Jiaotong University, Beijing, 100044, China
[b] TOPS lab, Department of Civil and Environmental Engineering, University of Wisconsin-Madison, 1415 Engineering Drive, Madison, WI 53706, United States of America

HIGHLIGHTS

- Passenger flow demand under congestion is predicted with big data.
- A radial basis function neural network with dynamic input layer is introduced.
- The proposed method outperforms other models illustrated by three scenarios.

ARTICLE INFO

Article history:
Received 5 August 2018
Received in revised form 3 July 2019
Accepted 8 July 2019
Available online 10 July 2019

Keywords:
Radial basic function network
Fuzzy c-mean clustering
Train timetable
Outbound volume
Passenger flow control

ABSTRACT

Short-term passenger flow prediction and passenger flow control are essential for managing congestion in metros. This paper proposes a new dynamic radial basis function (RBF) neural network to forecast outbound passenger volumes and improve passenger flow control. First, we adopt a train timetable to model passenger flow propagation and identify potential stations that substantially impact the outbound volumes of the target stations. As a result, we incorporate inbound volume, outbound volume, and the train timetable to avoid overfitting. Second, passenger flow control is considered to improve the prediction accuracy by adding passenger flow control coefficients to our model, which then attempts to specify the true influence of these potential stations during crowded times. Finally, we construct a dynamic input radial basis function neural network whose performance is illustrated by the following three scenarios: large passenger flow under passenger flow control during morning peak hours, evening peak hours under passenger flow control, and normal passenger flow without passenger flow control. Compared with the backpropagation neural network, the wavelet support vector machine and the K-nearest neighbor, the proposed method achieves the best prediction performance at a half-hour prediction time lag. The proposed method can also identify crucial stations and time periods 30 min in advance, which contributes when considering proactive passenger flow control to alleviate congestion during peak hours in metro networks.

1. Introduction

Metros play a key role in alleviating urban congestion, saving energy, and reducing exhaust emissions [1]. However, metro congestion occurs because the metro construction capacity cannot satisfy the rapidly increasing passenger flow demand [2]. The passenger flow distribution in metro networks is imbalanced, especially during peak hours [3].

As a result, managers must consider a passenger flow control method to have a practical way to manage the substantial demand in Chinese metros [4–6]. Reliable short term passenger flow prediction is crucial for alleviating congestion and designing effective passenger flow control strategies [7]. Therefore, the ability to predict short-term passenger flow is vital in resolving metro crowding problems.

Soft computing methods have contributed to human well-being, ecosystem stability [8,9], and the transportation field, such as transit network design and passenger flow control [10]. In recent years, many studies have focused on the applying soft computing algorithms to transportation, especially in metros. Some researchers have investigated metro short-term passenger flow prediction through two model categories: parametric and nonparametric. Parametric models are typical tools used for predicting short-term passenger flow and include methods such as gray prediction [11] and the autoregressive moving average

* Corresponding author.
E-mail addresses: hyli@bjtu.edu.cn (H. Li), 17120891@bjtu.edu.cn (Y. Wang), xxy@bjtu.edu.cn (X. Xu), Lingqiao.qin@wisc.edu (L. Qin), hzhang2@oberlin.edu (H. Zhang).

https://doi.org/10.1016/j.asoc.2019.105620
1568-4946/

[2,12]. Ni et al. [2] developed a hybrid seasonal integrated autoregressive moving average model to predict short-term passenger flow in the New York metro. Parametric models are accurate at predicting stationary passenger flows.

Nonparametric models have also been extensively applied to the prediction domain, especially for predicting short term passenger flow due to their ability to capture more features and rules from historical data than can parametric models. The nonparametric models include the support vector machine (SVM) [13], neural networks [14–17], and Bayesian networks [18]. Sun et al. [13] developed the wavelet support vector machine (Wavelet-SVM) method to predict the transfer volume of Line 1 to Line 4 in the Beijing metro and showed that the proposed method was more accurate than a traditional SVM. Roos et al. [18] combined a dynamic Bayesian network with an expectation maximization model to predict short-term passenger flow in the Paris metro based on incomplete historical data and showed that the Bayesian model was more accurate than the historical average and the last-observation-carried-forward method. Wei et al. [14] combined empirical mode decomposition with backpropagation (BP) neural networks to predict short-term passenger flows. The results showed that the accuracy of the BP neural networks was better than that of the Seasonal Autoregressive Integrated Moving Average model. Ryu et al. [19] combined a greedy search algorithm and the K-nearest neighbor (KNN) model to predict short-term California highway traffic flows based on mutual information. Meanwhile, deep learning and ensemble learning, including a deep neural network [20], deep convolutional neural network, deep recurrent neural network [21], deep belief network [22], and some ensemble structures [23], have also been adopted to predict passenger flows.

The RBF neural network has been widely used in passenger flow prediction because of its simple structure and optimal global approximation ability [24]. Yu et al. [25] adopted an improved artificial bee colony RBF to predict traffic intersection flow. Wang et al. [26] combined an RBF neural network and a least squares SVM to predict passenger flows at DongZhiMen station in the Beijing metro. Chen. [27] developed an improved RBF to predict traffic flows in big data environments. Li et al. [15] adopted the multiscale radial basis function network (MSRBF) to predict the outbound volumes of stations in the Beijing metro: the accuracy of the proposed model was the best among an SVM, a boosted random tree, and a single-scale radial basis function (RBF) neural network.

However, nonparametric models have some flaws for short-term passenger flow prediction. For example, neural networks cannot easily determine the initial input to generate faster model convergence, and the model inputs may cause overtraining [28]. To address this problem, we introduce the train timetable to determine the initial input. Passenger flow control is also considered in the prediction.

Neural networks have been widely used to establish the mathematical relationships of dynamic systems based on input and output data [24]. An RBF neural network with one hidden layer can approximate any continuous function to a prospective accuracy, making it the primary architectural choice for passenger flow prediction.

This study aims to forecast outbound passenger volumes for different scenarios. We propose an RBF neural network model to forecast the outbound volume under passenger flow control in the Beijing metro. To address the overfitting problem of the RBF model and improve the prediction accuracy, we also mine various data, including the train timetable, ridership data, and passenger flow control data. First, for a specific target station, the initial potential model inputs are determined based on the train timetable. Second, the final model inputs are selected from these potential inputs, which are closely related to passenger flow data at the target station via the criterion of generalized cross-validation (GCV) and the error reduction coefficient (ERR). Finally, we add parameters related to passenger flow control to the model to improve the prediction accuracy. As a result, the spatial–temporal range that influences the outbound passenger volume at the target station can be dynamically determined.

The main contributions of this study are as follows:

(1) Data from multiple sources are combined to predict the outbound volumes of stations based on the RBF method, which extends a previous study that predicted the outbound volumes of stations using the inbound volume only [15]. In addition to ridership, we employ the train timetable and passenger flow control in the proposed method. To avoid overfitting, the train timetable is used to determine the passenger flow propagation along station paths that have a strong effect on the outbound volume of the target station. We incorporate passenger flow control into our RBF to more precisely estimate the passenger volume that will be transferred to the target station.

(2) We predict the passenger flow demand under control. Passenger flow control is considered one of the most practical ways to reduce safety risks during peak hours in China [6,14,16]. However, the mechanism controlling the relationship between passenger flow control and passenger flow change is ambiguous; this study is the first attempt to predict passenger flows that considers passenger flow control.

(3) We introduce an RBF network with dynamic input to simplify the calculations and improve the prediction accuracy. In the case study, the root mean square error (RMSE) and mean absolute percentage error (MAPE) of the proposed method decreased by 37.9592%, 26.6422% and 15.4321% and by 23.5833%, 20.0855% and 21.8502%, respectively, compared with those of the BP neural network, the Wavelet-SVM and the KNN model, indicating that the proposed model achieves a better performance than do the other methods.

The remainder of this study is organized as follows: Section 2 presents the dynamic RBF neural network approach to predict short-term passenger flow. Section 3 describes the dataset adopted for the case study. Section 4 illustrates the prediction process under different scenarios and discusses the results. Finally, Section 5 presents the conclusions and suggestions for future research.

2. Methodology

2.1. NARX model

A multi-input/single-output nonlinear system (MISO) is proposed to describe the outbound volume prediction problem. The nonlinear autoregressive moving average method with exogenous inputs is used to model the MISO system as follows [29]:

$$y(t) = f(y(t-1), y(t-2), \ldots y(t-n_y), u_i(t-1), u_i(t-2), \ldots u_i(t-n_u), \varepsilon(t-1), \varepsilon(t-2), \ldots \varepsilon(t-n_\varepsilon)) + \varepsilon(t), \quad (1)$$

where $y(t)$ is the outbound volume of the target station predicted at time step t; $u_i(t)$ is the inbound volume of station i at time step$t$; f is an unknown nonlinear mapping function that usually links the output of the system to the inputs; n_y, n_u and n_ε are the maximum time lags in the previous outputs, inputs, and model errors, respectively; and $\varepsilon(t)$ is the model error at time step t. If the moving average noise is not considered, then Eq. (1) can be approximated to the NARX model, which is defined as follows:

$$y(t) = f(y(t-1), y(t-2), \ldots y(t-n_y), u_i(t-1), u_i(t-2), \ldots u_i(t-n_u)) + \varepsilon(t) \quad (2)$$

Let $X(t) = [X_1(t), X_2(t), \ldots X_d(t)]$, $d = n_y + n_u$, and

$$X_a(t) = \begin{cases} y(t-a) & 1 \le a \le n_y \\ u(t-(a-n_y)) & n_y + 1 \le a \le d \end{cases}.$$

The NARX model then can be expressed as follows:

$$y(t) = f(X(t)) + \varepsilon(t), \tag{3}$$

where f is an unknown nonlinear function that will be approximated by an RBF neural network.

2.2. RBF neural network

An RBF neural network is a three-layer neural network consisting of an input layer, a hidden layer, and an output layer. The input layer is denoted as an input vector (ridership data on different days), i.e., $x = \{x_1, x_2, \ldots, x_J\}$, where J is the number of model input terms. The hidden layer maps the input layer to a higher dimension with a RBF [30], in which the Gauss basis function is adopted as the radial basis function:

$$\varphi_i(x) = \exp(-\frac{\|x - c_i\|^2}{\sigma^2}), \forall i \in \{1, 2, 3, \ldots, I\}, \tag{4}$$

where $\|$ denotes the Euclidean distance, $c = \{c_1, c_2, \ldots c_I\}$ denotes the center set, I is the number of center terms, and σ is the scale of the basis function and is a known parameter. The output layer is a target vector used for prediction (i.e., outbound volume) and is calculated by a linear expression of the hidden layer:

$$y(t) = \omega\varphi \tag{5}$$

where $y = \{y_1, y_2, \ldots y_K\}$ is the predicted value, $\omega = \{\omega_1, \omega_2, \ldots \omega_L\}$ is a weight matrix, and $\varphi = \{\varphi_1, \varphi_2, \ldots \varphi_I\}$ is a regression matrix. The unknown parameters of the RBF neural network are the center set c and the weight matrix ω.

Algorithms that can address the unknown parameters include fuzzy c-means (FCM) and orthogonal least squares, the details of which are presented below.

(1) The fuzzy c-means (FCM) clustering algorithm is adopted to determine the center of the hidden layer. The key aspect of FCM is to make similar clusters have the highest similarity and different clusters have the smallest similarity [31]. The proposed objective function of this algorithm is to minimize the following function:

$$J_\gamma = \sum_{i=1}^{N_k} \sum_{j=1}^{N} \mu_{i,j}^{\gamma} \|x_j - c_i\|^2, \forall i \in \{1, 2, \ldots, I\}, j \in \{1, 2, \ldots, J\}, \tag{6}$$

where $\mu_{i,j}^{\gamma}$ denotes the membership degree value and $\|x_j - c_i\|^2$ denotes the Euclidean distance between the samples and the cluster centers. Note that the membership degree is subject to the constraint that the sum of the membership for all the classes is 1.

$$\sum_{i=1}^{N_k} \mu_{i,j}^{\gamma} = 1 \tag{7}$$

Using the Lagrange multiplier method, the membership degree $\mu_{i,j}^{\gamma}$ and the center c_i are calculated with a given number of clusters.

Another unknown parameter in FCM is the optimal number of clusters. To determine this parameter, a rule to minimize the absolute error of the prediction is adopted. Note that the absolute error of the prediction is the difference between the actual value and the predicted value, and it varies among different numbers of clusters.

(2) The orthogonal least squares (OLS) algorithm is applied to determine the weight of the RBF. If orthogonal triangulation is performed, Eq. (5) is formulated as follows:

$$y = \varphi\omega = UA\omega, \tag{8}$$

where A is an upper triangulation matrix and U is an orthogonal matrix. Note that A and U can be determined solely by φ.

If U^T is introduced on both sides of Eq. (8), the following equation is obtained:

$$U^T y = U^T UAw = HAw = Hg, \tag{9}$$

therefore, g and ω are solved as follows:

$$g = H^{-1}U^T y \tag{10}$$

$$\omega = A^{-1}g = A^{-1}H^{-1}U^T y \tag{11}$$

2.3. Model structure selection based on train timetable

2.3.1. Notations

The time period H is dispersed into finite time intervals, denoted by M. Here, τ is an interval duration that satisfies the formula $\tau M = H$, and *m is a time interval with length τ such that* $1 \le m \le M$. For generality, the time interval is the main unit of time in this paper, and τ is assumed to be 30 min. The following notations are defined to formulate the proposed model:

Sets

L	Set of lines
S	Set of all stations indexed by i
SS	Set of predicted stations indexed by p
S_p	Set of all stations, except station p
K	Set of trains indexed by k
$S'_p(m)$	A subset of S_p whose inbound volumes are considered as the initial input for predicting station p at interval m considering ϕ time tags
$S_f(m)$	A subset of $S'_p(m)$ whose inbound volumes are considered as the final input for predicting station p at interval m considering ϕ time tags

Parameters

$AT_k(i)$	Arrival time of train k at station i, $i \in S$
$DT_k(i)$	Departure time of train k at station i, $i \in S$
$RT_{i,j}^k$	Running time of train k from station i *to station* j, $i, j \in S$
$RT_{i,j}$	Average running time from station i to station j, $i, j \in S$
$\eta_i^p(m)$	Maximum time lag for a train from station i to arrive at target station p *during interval* m, $i \in S_p$, $p \in SS$
$In_i(m)$	Inbound volume of station i during interval m
$Out_i(m)$	Outbound volume of station i during interval m
ϕ	A constant that denotes the number of time lags
$\delta_\beta(m)$	Passenger flow control proportion for inbound volume of station β during interval m

2.3.2. Model structure selection

Model structure selection is an important step to improve the prediction accuracy of an RBF neural network [32]. We take a line in L as an example to explain the model structure selection process. Model structure selection is based on the train timetable data. An example of a train timetable is shown in Table 1. The train timetable provides the arrival and departure times of a train at the stations it serves. Table 1 lists the train code, station name, arrival time and departure time of a train. We can calculate the average running time for the train between two stations from the train timetable.

The model structure selection steps are as follows:

(1) Calculate the average running time from station i ($i \in S_p$) to the target station p($p \in SS$), denoted as follows:

$$RT_{i,p}^k = AT_k(p) - DT_k(i), \forall k \in K \tag{12}$$

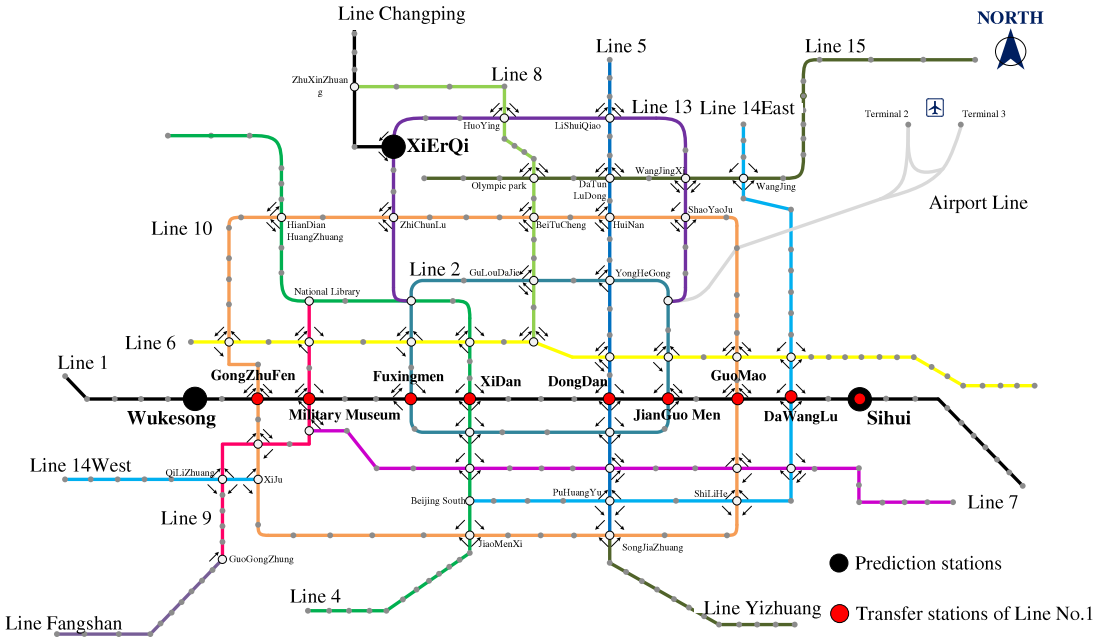

Fig. 1. Beijing metro map and predicted stations.

Table 1
Train timetable data.

Train code	Jianguomen		Yonganli		Guomao	
	Arrivaltime	Departure time	Arrival time	Departure time	Arrival time	Departure time
651106	8:46:00	8:46:30	8:48:30	8:49:30	8:50:30	8:51:00
201108	8:50:30	8:51:30	8:53:00	8:53:30	8:54:30	8:55:30

$$RT_{i,p} = \frac{1}{K}\sum_{k} RT^{k}_{i,p}. \tag{13}$$

(2) Calculate $\eta^p_i(m)$ for each station i in set S_p to the target station p during interval m as determined by the following:

$$\eta^p_i(m) = \begin{cases} 1 & if\ RT_{i,p} < \tau \\ 2 & if\ \tau \le RT_{i,p} < 2\tau \\ 3 & if\ 2\tau \le RT_{i,p} < 3\tau \\ \cdots\cdots & \\ n & if\ (n-1)\tau \le RT_{i,p} < n\tau \end{cases}, \tag{14}$$

where $\eta^p_i(m)$ is the maximum time lag in the prediction for station i during time interval m. Station i will be excluded from S_p at interval m if $\eta^p_i(m) > \phi$, that is, $S'_p(m) = S_p - \{i|\eta^p_i(m) > \phi, \forall i \in S_p\}$. Thus, the initial model input is

$x_{ini} = \{In_r(m - \eta^p_r(m)) \,|\, \forall r \in S'_p(\mathrm{m})\} \cup \{Out_p(m-1)\}$.

(3) The final model inputs are selected according to GCV and ERR from $S'_p(m)$. The GCV method is used to determine the optimal number of inbound volume inputs n^*_c as suggested by [33]:

$$n^*_c = \underset{n_c}{\operatorname{argmin}}\, GCV(n_c)$$
$$st., \quad GCV(n_c) = \left(\frac{N}{N-\lambda n_c}\right)^2 MSE(n_c), \forall n_c \in [0, N], \tag{15}$$

where MSE denotes the mean square error, N denotes the sample size (the number of elements in set $S'_p(m)$), and n_c is the number of model input vectors. For the RBF model, the input vector is expressed as $x = \{x_1, x_2, \ldots, x_J\}$ in Section 2.2, and J is formulated as $J = n^*_c + 1$. Note that λ is a constant obtained through the following equation:

$$\lambda = \max\{1, \rho N\}, \forall 0 \le \rho \le 0.01. \tag{16}$$

To determine the inbound volumes, the ERR value for each station in $S'_p(m)$ is calculated as in [34]:

$$ERR = \frac{(y^T U_i)^2}{(y^T y)\cdot(U_i^T U_i)}, \tag{17}$$

where U_i is a column of the orthogonal matrix U in Formula (8).

The ERR values of each station in $S'_p(m)$ are sorted from large to small, and the first n^*_c stations that correspond to the inbound volume of the target station are selected. This set of stations is denoted as $S_f(m)$. The final model input is expressed as

$x_{final} = \{IN_\beta(m - \eta^p_\beta(m)) \,|\, \forall \beta \in S_f(m)\} \cup \{Out_p(m-1)\}$.

2.4. Dynamic input model under passenger flow control

If passenger flow control is considered, the number of passengers that arrives at the target station is different from the inbound volume collected through smart cards during a given timespan. Thus, the components of the model input x_{final} must be dynamic to consider passenger flow control. The procedures for determining the model input are shown below.

(1) To predict the outbound volume of station p during time interval m, the stations in set $S_f(m)$ that implement passenger flow control must be identified; that is, we must determine whether each final model input x_{final} implements passenger flow control on the inbound volume of station $\beta, \forall \beta \in S_f(m)$ during time interval $m - \eta^p_\beta(m)$.

(2) When the inbound volume of station β is controlled during the time interval $m - \eta^p_\beta(m)$, $\delta_\beta(m - \eta^p_\beta(m)) < 1$; otherwise, $\delta_\beta(m - \eta^p_\beta(m)) = 1$.

(3) The final model input is updated by

$$x_{final} = \{\delta_\beta(m-\eta^p_\beta(m))IN_\beta(m-\eta^p_\beta(m)) \,|\, \forall \beta \in S_f(m)\} \cup \{Out_p(m-1)\}.$$

Table 2
Station name abbreviations for Line Changping and Line 1.

Station name	Abbreviation	Line	Station name	Abbreviations	Line
Nanshao	NS	Changping	Shahegaojiaoyuan	SHGJY	Changping
Shahe	SHE	Changping	Gonghuacheng	GHC	Changping
Zhuxinzhuang	ZXZ	Changping	Shengmingkexueyuan	SMKXY	Changping
Xierqi	XRQ	Changping	Pingguoyuan	PGY	1
Gucheng	GC	1	Bajiaoyouleyuan	BJYLY	1
Babaoshan	BBS	1	Yuquanlu	YQL	1
Wukesong	WKS	1	Wanshoulu	WSL	1
Gongzhufen	GZF	1	Junshibowuguan	JSBWG	1
Muxidi	MXD	1	Nanlishilu	NLSL	1
Fuxingmen	FXM	1	Xidan	XD	1
Tiananmenxi	TAMX	1	Tiananmendong	TAMD	1
Wangfujing	WFJ	1	Dongdan	DD	1
Jianguomen	JGM	1	Yonganli	YAL	1
Guomao	GM	1	Dawanglu	DWL	1
Sihui	SH	1	Sihuidong	SHD	1

Table 3
Part of the passenger flow control schedule in the Beijing metro.

Line	Station name	Passenger flow control time period
1	SH	07:00–09:00 and 16:00–20:00
1	FXM	17:00–18:45
1	PGY	06:50–08:30
1	GC	06:50–08:50
1	SHD	07:00–09:30
1	BBS	07:00–08:30
1	BJYLY	06:50–08:30
1	YAL	18:00–19:00
Changping	XEQ	07:00–09:00 and 17:00–19:30

3. Data source

This study adopts multisource data to predict passenger volume at metro stations. The predictions for the Xierqi, Sihui, and Wukesong stations in the Beijing metro are shown in Fig. 1, which introduces the layout of the Beijing metro network. The lines represent metro lines, and the points represent metro stations. The target prediction stations are denoted by black circles: the nine transfer stations of Line 1 are denoted by the red circles in Fig. 1.

These stations were selected for two reasons

(1) The Xierqi and Sihui stations are transfer stations that implement passenger flow control during peak hours. In particular, the Xierqi station has a large passenger flow volume during the morning peak hours.

(2) The Wukesong station has a constant large passenger flow because it is located in a business district. Note that the station names and their abbreviations for the Changping Line and Line 1 are shown in Table 2, which lists the station name, the lines to which it belongs and the corresponding abbreviation. Note that most of the stations in Table 2 are invisible in Fig. 1 as to keep the figure clear.

We employ three types of data sources. The first data source consists of ridership data collected from smart cards that reflects the inbound and outbound volume of all stations at 30-minute intervals. We considered the ridership data from February 12th, 2015 to March 3rd, 2015. The outbound volumes for each 30-minute interval on March 3rd form the prediction targets, as shown in Fig. 2. The blue dotted line represents the outbound volumes from the Xierqi station, which has a large passenger flow during morning peak hours. Unlike Xierqi station, the green line denotes the outbound volume of the Sihui station, while the red dotted line denotes the outbound volume of Wukesong station, and these represent normal passenger flow and passenger flow control.

The second data source is the train timetable, which provides train arrival and departure times for a station. Here, we adopt the train timetable data for Line 1 and Line Changping were sourced from the Beijing Metro Traffic Control center. The partial transit schedules for Line 1 and Line Changping from 07:30 to 08:30 are shown in Fig. 3, which illustrates the arrival and departure times for trains at stations. The horizontal axis of Fig. 3 represents time, while the vertical axis shows the station names. The red lines connecting two stations denote the train moving from one station to another after a certain period of time.

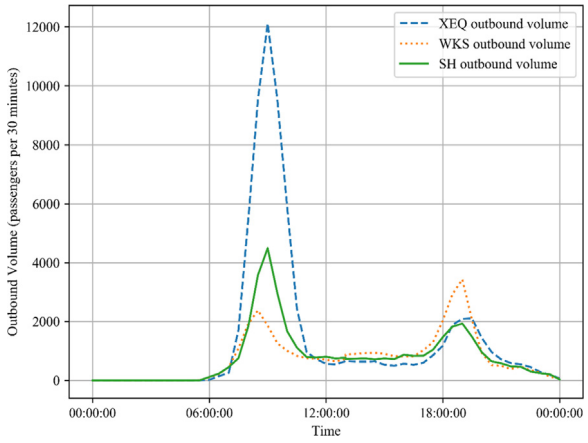

Fig. 2. Passenger flow fluctuations at target stations on March 3rd, 2015.

The third data source consists of information about passenger flow control in the Beijing metro sourced from the Beijing metro website. This data source contains the stations and the time periods during which passenger flow control is implemented, as shown in Table 3. Passenger flow control requires excess passengers to queue at fixed facilities; after waiting a short time, they are allowed to enter the metro system [6]. This source lists the times and stations at which passenger flow control was implemented. Because some passengers may fail to board a train under passenger flow control, the model inputs should be altered based on this data.

4. Experimental results

In this section we report on the three scenarios shown in Table 4 developed to verify the accuracy of the proposed dynamic RBF model. Table 4 shows the station names, prediction variables and prediction scenarios. The three typical stations have different scenarios but the same prediction variables. The scenarios are designed by varying the following two dimensions: (1) the passenger flow volume and (2) whether passenger flow control measures are implemented. Based on these two dimensions, our

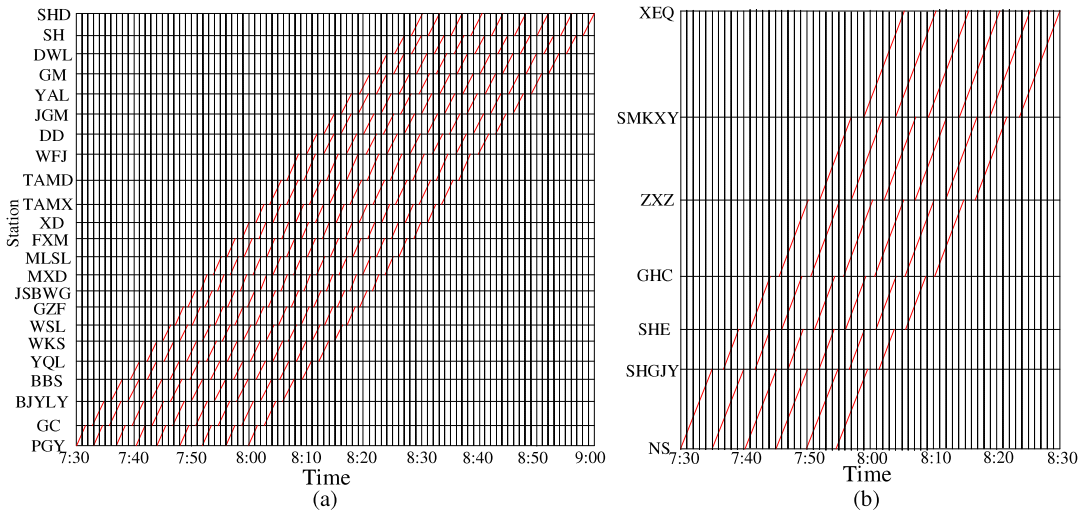

Fig. 3. Partial transit schedules for two lines from 07:30–08:30: (a) Line 1; (b) Line Changping.

Table 4
Prediction stations and corresponding scenarios.

Station	Prediction variable	Scenario
XEQ	Outbound volume	Large passenger flow under passenger flow control during morning peak hours
WKS	Outbound volume	Normal passenger flow
SH	Outbound volume	Peak hours under passenger flow control

model predicts the outbound passenger volume of the three stations.

First, the outbound volume of the XEQ station, which has a high passenger volume during morning peak hours and implements passenger flow control is predicted. Second, the outbound volume of the WKS station with normal passenger flow is predicted. Finally, the outbound volume of the SH station under passenger flow control during peak hours is predicted.

We adopt the MAPE, the variance of absolute percentage error (VAPE), and RMSE to evaluate the accuracy of the prediction results [35,36]. These metrics are calculated as follows:

$$MAPE = \frac{1}{O}\sum_{i=1}^{N}\frac{|y_i - \hat{y}_i|}{\bar{y}} \cdot 100\% \tag{18}$$

$$VAPE = \frac{1}{O}\sum_{i=1}^{N}(e_i - \bar{e})^2 \cdot 100\% \tag{19}$$

$$RMSE = \sqrt{\frac{1}{O}\sum_{i=1}^{N}(y_i - \hat{y}_i)^2}, \tag{20}$$

where O is the number of observational vectors; $y = \{y_1, y_2, y_3, \ldots, y_O\}$ represents the real passenger flow values; $\hat{y} = \{\hat{y}_1, \hat{y}_2, \hat{y}_3, \ldots, \hat{y}_O\}$ represents the predicted passenger flow values; $e = \frac{|y-\hat{y}|}{y}$ is the absolute error; $\bar{e}$ is the average absolute error; and $e_i = \frac{|y_i-\hat{y}_i|}{y_i}$ represents the absolute error at the ith time lag prediction.

4.1. Outbound passenger flow prediction of XEQ station

The XEQ station is the origin station of Line Changping and has a large passenger flow during the morning peak hours. The outbound volume exceeds 10,000 passengers during most peak half-hour periods. Identifying the stations that significantly impact the passenger flow to the XEQ station during a specific time period is critical for managing the large number of passengers. Thus, we selected one day (i.e., February 3rd, 2015) and predicted the outbound volume every 30 min.

4.1.1. Prediction process

First, the train running times from other stations to the XEQ station are calculated according to the train timetable for Line Changping in Fig. 3. The average running times from the NS, SHGJY, SHE, GHC, ZXZ, and SMKXY stations to the XEQ station are 25 min, 20 min, 17 min, 14 min, 10 min, and 6 min, respectively. The longest running time for the trip is from the NS station to the XEQ station, and it is less than the time lag τ in the prediction; that is, the outbound volumes and inbound volumes of all stations on Line Changping should be taken as the model input to the XEQ station. Thus, the initial model input is a matrix composed of the inbound and outbound volumes denoted as

$$\mathbf{x_{XEQ}}(m) = \{y_{\mathbf{XEQ}}(m-1), x_{\mathbf{NS}}(m-1), x_{\mathbf{SHGJY}}(m-1), x_{\mathbf{SHE}}(m-1), x_{\mathbf{GHC}}(m-1), x_{\mathbf{ZXZ}}(m-1), x_{\mathbf{SMKXY}}(m-1)\},$$

where $y_{\mathbf{XEQ}}(m-1)$ is the outbound volume vector of the XEQ station during time interval $m-1$ trained for 19 days, and $x_{\mathbf{NS}}(m-1)$, $x_{\mathbf{SHGJY}}(m-1)$, $x_{\mathbf{SHE}}(m-1)$, $x_{\mathbf{GHC}}(m-1)$, $x_{\mathbf{ZXZ}}(m-1)$, $x_{\mathbf{SMKXY}}(m-1)$ denotes the inbound volume vectors of the NS, SHGJY, SHE, GHC, ZXZ, and SMKXY stations, respectively, during time interval $m-1$ trained for 19 days. The number of model input vectors n_c^* is calculated by Eq. (15): its value is 6. Thus, the six model input terms in addition to $y_{\mathbf{XEQ}}(m-1)$, (that is, the initial model input) are expressed as follows:

$$\mathbf{x_{XEQ}}(m) = \{y_{\mathbf{XEQ}}(m-1), x_{\mathbf{NS}}(m-1), x_{\mathbf{SHGJY}}(m-1), x_{\mathbf{SHE}}(m-1), x_{\mathbf{GHC}}(m-1), x_{\mathbf{ZXZ}}(m-1), x_{\mathbf{SMKXY}}(m-1)\}.$$

Passenger flow control is considered at the XEQ station only from 07:00–09:00 and from 17:00–19:30. The passenger flow control information is not considered when updating the final input terms. Thus, in this prediction time lag, the final model input is expressed as follows:

$$\mathbf{x_{XEQ}}(m) = \{y_{\mathbf{XEQ}}(m-1), x_{\mathbf{NS}}(m-1), x_{\mathbf{SHGJY}}(m-1), x_{\mathbf{SHE}}(m-1), x_{\mathbf{GHC}}(m-1), x_{\mathbf{ZXZ}}(m-1), x_{\mathbf{SMKXY}}(m-1)\}.$$

The center of FCM and the optimal number of clusters are determined at all prediction time lags. The optimal number of clusters is selected by the minimum absolute error. For our RBF model, different prediction time lags often have different optimal

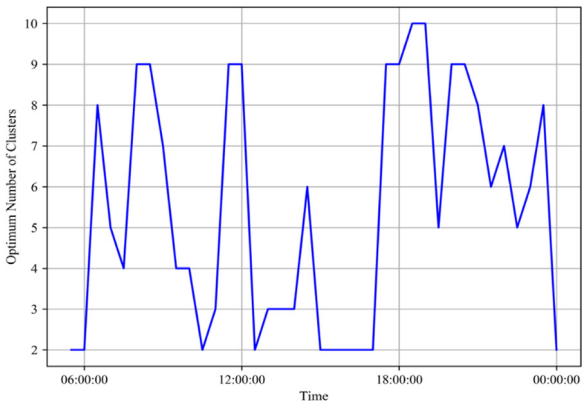

Fig. 4. Optimum numbers of clusters at different time lags for the XEQ station.

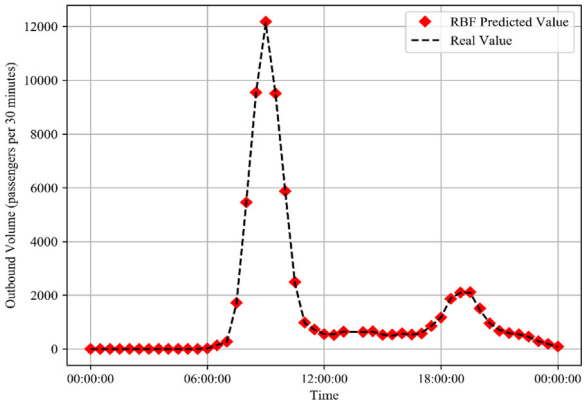

Fig. 5. Real volume and predicted outbound volumes of the XEQ station on March 3rd, 2015.

numbers of clusters. The numerous scattered points of the optimal number of clusters at different time lags for the XEQ station are illustrated in Fig. 4. The values on the blue line at different prediction time lags denote the different optimal numbers of clusters. For an RBF neural network, different clusters indicate that the hidden layer is dynamic at different time lags. Note that the parameter settings for the training process are proposed in Section 4.4.

4.1.2. Prediction results

The obtained prediction results are shown in Fig. 5, where the prediction values are very similar to the real values. The horizontal axis represents the prediction time lag, and the vertical axis represents the outbound volume of passenger flow. The dotted line represents the real values of the XEQ station on March 3rd, 2015, and the red diamonds represent our predicted values. The RMSE, MAPE, and VAPE of the prediction for the XEQ station are 21.1225, 0.8004, and 2.5294×10^{-5}, respectively. We can conclude that RBF performs well in predicting the outbound volume of the XEQ station in all time lags.

We describe the model prediction performance with the help of the absolute error and relative error metrics. The absolute error and relative error for the XEQ station at different time lags are shown in Fig. 6. Our RBF model achieves good performances at all time lags for XEQ prediction even though some bad performances seemingly occur during several time periods. On one hand, the relative error seems large because the passenger flow volume during these two time lags (06:00 and 00:00) is small. On the other hand, the absolute error is relatively large, while the relative error is small in the morning peak hour and evening peak hour. Thus, these poor time lag performances can be exclusive.

The final prediction results concluded that the outbound volumes of all the other stations on Line Changping are closely related to those of the XEQ station, as shown in Fig. 5. To control the outbound volume of the XEQ station, passenger flow control should be considered in the NS, SHGJY, SHE, GHC, ZXZ, and SMKXY stations 30 min in advance, which is the time required for passengers to travel from these stations to the XEQ station. For example, the peak half-hour for the XEQ station is 08:30–09:00, when the maximum outbound volume is 12,122 passengers per hour. Thus, passenger flow control for the inbound volume at the NS, SHGJY, SHE, GHC, ZXZ, and SMKXY stations should be considered from 08:00–08:30.

4.2. Outbound passenger flow prediction of WKS station

The WKS station is a representative station in Beijing Metro Line 1 because it is surrounded by shopping malls. Compared with the previous prediction of the XEQ station, the location of the WKS station attracts large passenger volumes and has a more complicated setup.

The outbound volume from the WKS station without passenger flow control is predicted at every 30-minute interval from 04:30 to 24:00 on February 13th, 2015. Line 1 of the Beijing metro has nine transfer stations (denoted by circles in Fig. 1), where the inbound volume and the transfer volume are considered as model inputs.

4.2.1. Prediction process

First, the train running times from other stations to the WKS station are calculated based on the timetable for Line 1 in Fig. 3.

To predict the outbound volume from the WKS station during time interval m, we selected the inbound volumes for the stations on Line 1 during the time interval $m-1$ for which the train running time to the WKS station does not exceed τ. For those stations where the train running time to the WKS station ranges between τ and 2τ, the outbound volumes during time period $m-2$ are selected as the initial model input. For stations on Line 1, the train running times from the PGY, GC, BJYLY, BBS, YQL, WSL, GZF, JSBWG, MXD, NLSL, FXM, XD, TAMX, TAMD, WFJ, DD, JGM, and YAL to the WKS station do not exceed τ; thus, the inbound volumes of these stations during time interval $m-1$ are selected as the initial model input. The train running times from the GM, DWL, SH, and SHD stations to the WKS station are between τ and 2τ; thus, the inbound volumes of these stations during time interval $m-2$ are selected as the initial input.

The result is that the initial model is a matrix consisting of inbound and outbound volumes during different time periods during 19 days of training. The prediction during the 05:00–05:30 time interval of the WKS station is used to show the selected model input terms. According to Eq. (15), n_c^* is 9. Ten model input terms are selected according to the ERR value for the different initial model input terms as shown in Table 5, which lists the model input terms and the corresponding ERR values. For Line 1, the SH, FXM, PGY, GC, SHD, BBS, BJYLY, and YAL stations must consider the controlled proportion of passenger flow. Therefore, the final model input is

$$\begin{aligned}\mathbf{x}^{\mathbf{f}}_{\mathbf{WKS}}(m) = \{&\delta_{PGY}(m-1)x_{PGY}(m-1), x_{BJYLY}(m-1),\\ &x_{YQL}(m-1), \delta_{BBS}(m-1)x_{BBS}(m-1),\\ &x_{WSL}(m-1), x_{GZF}(m-1), x_{JSBWG}(m-1),\\ &\delta_{FXM}(m-1)x_{FXM}(m-1), x_{WKS}(m-1)\}.\end{aligned}$$

The center of FCM and the optimal number of clusters are determined. The optimal number of clusters is selected by the

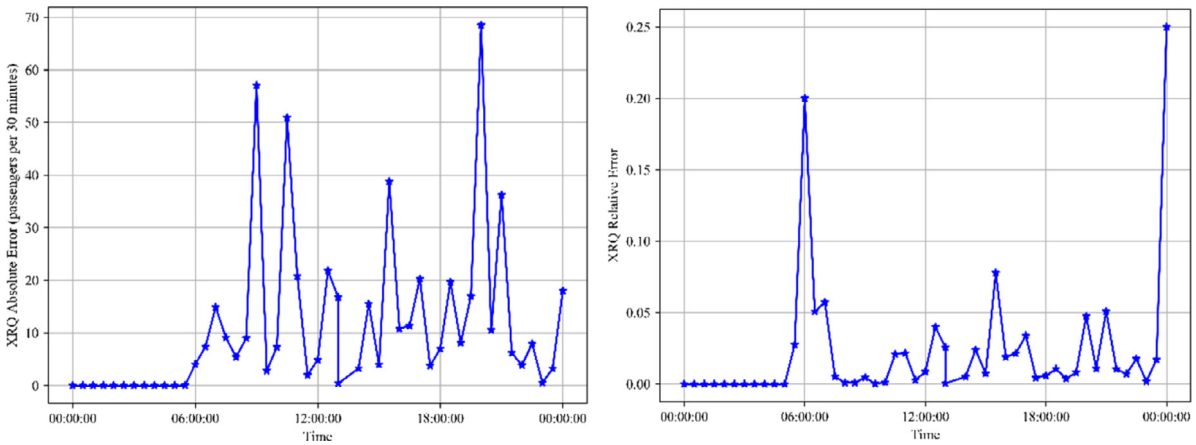

Fig. 6. RBF absolute errors and relative errors for the XEQ station predictions.

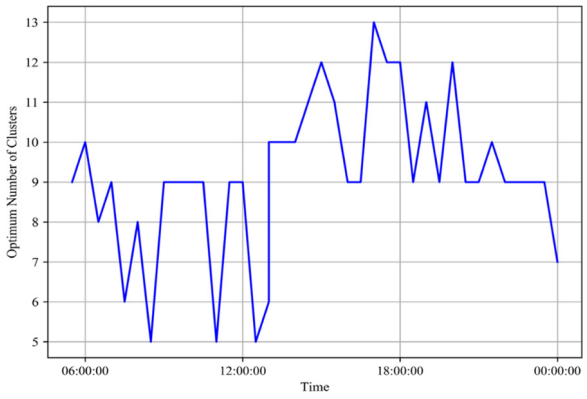

Fig. 7. Optimum number of clusters for the WKS station at different time lags.

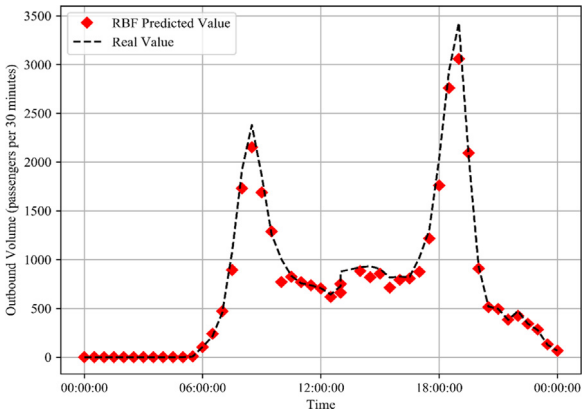

Fig. 8. Real outbound volume and predicted outbound volume of the WKS station on March 3rd, 2015.

Table 5
Selected model input terms and the ERR values of passenger flow predictions for the WKS station.

Model input term	ERR value
Inbound volume of PGY (04:30–05:00)	0.7148
Inbound volume of BJYLY (04:30–05:00)	0.0929
Inbound volume of YQL (04:30–05:00)	0.0168
Inbound volume of BBS (04:30–05:00)	0.0126
Inbound volume of WSL (04:30–05:00)	0.0413
Inbound volume of GZF (04:30–05:00)	0.0346
Inbound volume of JSBWG (04:30–05:00)	0.0391
Inbound volume of FXM (04:30–05:00)	0.0353
Outbound volume of WKS (04:30–05:00)	0.0021

minimum absolute error. As a result, the optimal number of clusters at the WKS station at different time lags is obtained, as shown in Fig. 7. The horizontal axis of Fig. 7 represents the prediction time lag, and the vertical axis represents the optimal number of clusters. The values on the blue line at different prediction time lags reflect the different optimal numbers of clusters, which proves that different optimal numbers of clusters should be considered at different time lags.

4.2.2. Prediction results

The prediction results of the dynamic RBF model are presented in Fig. 8. The horizontal axis represents the prediction time lag, and the vertical axis represents the outbound passenger flow volume. The dotted line denotes the real values of the WKS station on March 3rd, 2015, and the red diamonds represent the predicted values of our model. The proposed RBF model provides accurate predictions of the outbound volume of the WKS station at almost all time lags. The RMSE and MAPE of the prediction are 112.9727 and 7.4200, respectively.

The absolute error and relative error of RBF in the WKS station are shown in Fig. 9. Our RBF model performs well for nearly all time lags except at the end of the morning peak hour. During that time segment, both the absolute error and the relative error are relatively large.

According to the final prediction result in Fig. 8 and the final model inputs in Table 5, the inbound volumes of the PGY, BJYLY, YQL, BBS, WSL, GZF, JSBWG, and FXM stations on Line 1 are closely related to the outbound volume of the WKS station. Therefore, to control the outbound volume of the WKS station, passenger flow control measures should be implemented at the PGY, BJYLY, YQL, BBS, WSL, GZF, JSBWG, and FXM stations 30 min in advance. For example, 18:30–19:00 is in the peak period for the WKS station when the outbound volume is 3428 passengers/hour. Thus, passenger flow control measures for the inbound volume should be considered from 18:00–18:30 in the PGY, BJYLY, YQL, BBS, WSL, GZF, JSBWG, and FXM stations.

4.3. Outbound passenger flow prediction of SH

In this section, we predict the passenger flow at the SH station during the evening peak hour under passenger flow control. The data from February 12th, 2015 to March 2nd, 2015 are considered as the training dataset; data are collected every half hour from 04:30 to 24:00.

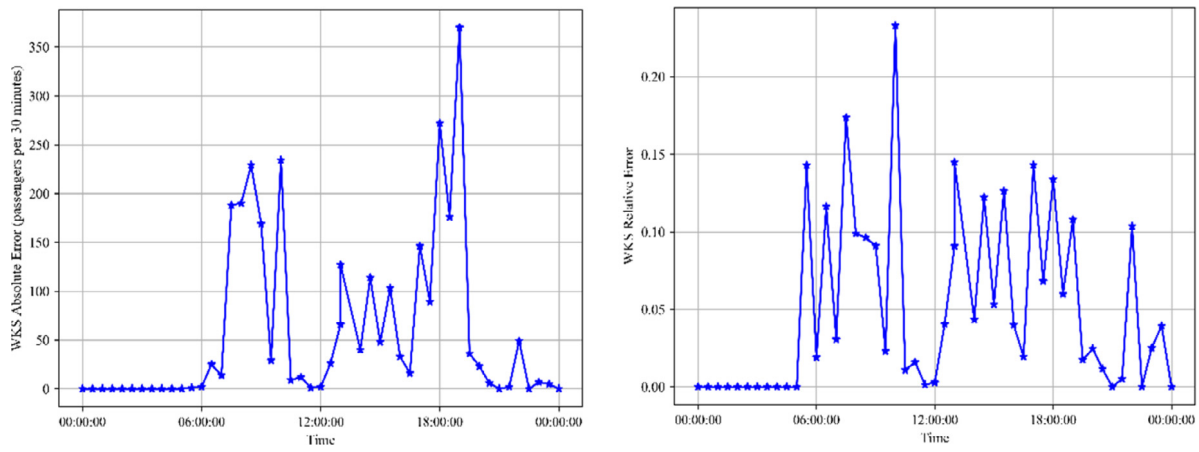

Fig. 9. RBF absolute error and relative error of predictions for the WKS station.

4.3.1. Prediction process

First, the train running times from other stations to the SH station are calculated based on the timetable for Line 1 as shown in Fig. 3. This process for determining the initial model input is the same as that used for the prediction process at the WKS station. The train running times from the SHD, DWL, GM, YAL, JGM, DD, WFJ, TAMD, TAMX, XD, FXM, NLSL, MXD, and JSBWG stations to the SH station do not exceed τ, and the train running times from the GZF, WSL, WKS, YQL, BBS, BJYLY, GC, and PGY station to the SH station are between τ and 2τ. Thus, the initial model input is expressed as follows:

$$\begin{aligned}\mathbf{x_{SH}}(m) = \{&y_{SH}(m-1), x_{PGY}(m-2), x_{GC}(m-2),\\ &x_{BJYLY}(m-2), x_{BBS}(m-2), x_{YQL}(m-2),\\ &x_{WKS}(m-2), x_{WSL}(m-2), x_{GZF}(m-2), x_{JSBWG}(m-1),\\ &x_{MXD}(m-1), x_{NLSL}(m-1),\\ &x_{FXM}(m-1), x_{XD}(m-1), x_{TAMX}(m-1), x_{TAMD}(m-1),\\ &x_{WFJ}(m-1), x_{DD}(m-1),\\ &x_{JGM}(m-1), x_{YAL}(m-1), x_{GM}(m-1),\\ &x_{DWL}(m-1), x_{SHD}(m-1)\}.\end{aligned}$$

The prediction during the 06:30–07:00 time interval of the SH station is used to show the selected model input terms. Next, n_c^* is calculated as 7 using Eq. (15). Eight model input terms are selected, as shown in Table 6, which lists the model input terms and corresponding ERR values. Note that passenger flow control is considered in the model input. For Line 1, the SH, FXM, PGY, GC, SHD, BBS, BJYLY, and YAL stations must consider the passenger flow control proportion. Thus, the final model input is expressed as follows:

$$\begin{aligned}\mathbf{x_{SH}^f}(m) = \{&\delta_{SHD}(m-1)x_{SHD}(m-1), y_{SH}(m-1),\\ &x_{DWL}(m-1), x_{GM}(m-1),\\ &x_{JGM}(m-1), x_{DD}(m-1), x_{WFJ}(m-1), x_{XD}(m-1)\}\end{aligned}$$

The center of FCM and the optimal number of clusters are determined. As noted in the previous section, different optimum numbers of clusters at the SH station are obtained during different time periods, as shown in Fig. 10, where the blue line at different prediction time lags denotes the different optimal numbers of clusters. The different optimal number of clusters represents the dynamic hidden layer of our RBF model.

4.3.2. Prediction results

The prediction results in Fig. 11 show that RBF performs well at predicting the outbound volume of the SH station in all the time lags. The horizontal axis denotes the prediction time lag, and the vertical axis denotes the outbound volume of the SH station. The dotted line represents the real values of the SH station on March 3rd, 2015, and the red diamonds represent the predicted values. The RMSE of the prediction is 46.6284, and the MAPE of the prediction is 3.5500.

The absolute error and relative error of RBF for the SH station are shown in Fig. 12 to reflect the performance of the model during all prediction time lags. Our model performs well in nearly all time lags except for the time segment around the time lag of 12:00. In that time segment, both the absolute error and relative error are relatively large and occurs because of a large change in passenger demand: before 12:00, a morning peak occurs with a large passenger flow, while after 12:00, passenger flow forms a plane due to the small demand at this station during the 12:00 time lag.

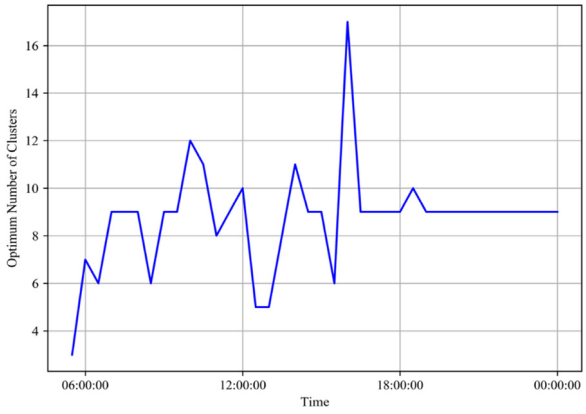

Fig. 10. Relationship between the numbers of clusters and the absolute errors of the SH station.

Table 6
Selected model input terms and the ERR when predicting passenger flow for the SH station.

Model input term	ERR value
Inbound volume of SHD (06:00–06:30)	0.9154
Outbound volume of SH (06:00–06:30)	0.0166
Inbound volume of DWL (06:00–06:30)	0.0311
Inbound volume of GM (06:00–06:30)	0.0229
Inbound volume of JGM (06:00–06:30)	0.0028
Inbound volume of DD (06:00–06:30)	0.0054
Inbound volume of WFJ (06:00–06:30)	0.0038
Inbound volume of XD (06:00–06:30)	0.0092

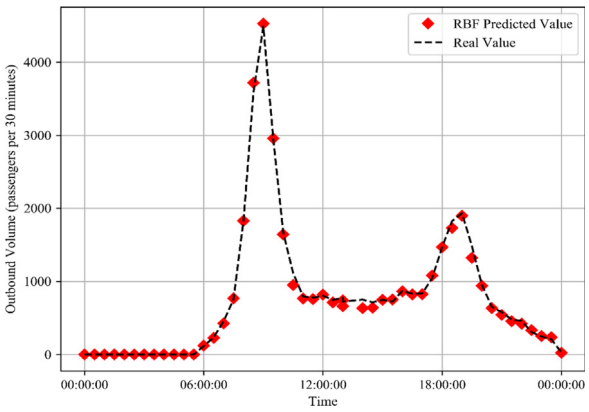

Fig. 11. Real outbound volume and predicted outbound volume for the SH station on March 3rd, 2015.

From the final prediction results in Fig. 11 and the final model input terms in Table 6, we can conclude that the inbound volumes of the SHD, DWL, GM, JGM, XD, DD, and WFJ stations on Line 1 are closely linked with the outbound volume of the SH station. To control the outbound volume of the SH station, passenger flow control measures should be implemented at the SHD, DWL, GM, JGM, XD, DD, and WFJ stations 30 min in advance because passengers leaving these stations usually arrive at the SH station within 30 min. For example, the most intense half-hour peak for the WKS station is 08:30–09:00: the outbound volume during that half-hour is 4489 passengers. Thus, passenger flow control measures should be considered to control the inbound volume from 08:00–08:30 at the SHD, DWL, GM, JGM, XD, DD, and WFJ stations.

4.4. Hyperparameter settings and time complexity analyses

Early-stopping is a common strategy for avoiding overfitting [37]. In the RBF neural network, both regularization and early-stopping can avoid overfitting. We take the 08:30–09:00 time interval as an example to demonstrate the early-stopping process. To avoid overfitting, a validation-based early-stopping method is adopted. The method halts the training process when the validation set loss does not decrease after training. To set the hyperparameters of the method, we used a grid search to find the parameters that lead to the best prediction performance. During model training, we randomly select 20% of the dataset as the validation dataset. Fig. 13 shows the training loss and validation loss for the XEQ and WKS stations: the vertical axis denotes the RBF loss, the blue line denotes the training loss, the red line denotes the validation loss and one epoch denotes one learning process over all training datasets. The best epochs of model training are 1210 (XEQ station) and 901 (WKS station).

Our model includes two processes: FCM clustering and the RBF training process. For FCM clustering, assume that m_1 denotes the number of samples, m_2 denotes the number of features, and k denotes the number of iterations. In Section 2.2, we used I to denote the number of center terms, that is, the number of neurons in the hidden layer, and used J to denote the model input terms, that is, the number of neurons in the input layer. Our RBF has one neuron in the output layer. The RBF of the hidden layer uses a square operation. Thus, the time complexity of FCM clustering is $O(km_1m_2I)$, and the time complexity of the RBF process is $O((IJ)^2 + I)$. Therefore, the total time complexity can be expressed as $O((IJ)^2 + I) + O(km_1m_2I) \approx O(n^2)$.

Table 7
The MAPE values of the XEQ, WKS, and SH stations.

MAPE	BP	Wavelet-SVM	KNN	RBF
XEQ	4.6783	4.4698	2.4551	0.8004
WKS	9.3625	8.3481	10.1222	8.7656
SH	6.6117	4.2408	4.8666	4.0662

Table 8
The VAPE values of the XEQ, WKS, and SH stations.

VAPE	BP	Wavelet-SVM	KNN	RBF
XEQ	2.9451	1.5893	0.6256	0.2457
WKS	0.9727	2.7595	1.7143	0.4357
SH	21.4034	4.5810	1.3540	0.2619

4.5. Model comparisons

To evaluate the performances of the dynamic RBF, the BP neural network, the Wavelet-SVM, and the KNN models, absolute error, relative error, and three other indexes of prediction accuracy are employed in this study. The BP neural network contains two hidden layers, each containing 10 neurons, and uses ReLU as the transfer function and the Adaptive Moment Estimation (Adam) as the optimizer. Wavelet-SVM takes the radial basis function as the kernel function and includes two layers of wavelet decomposition. KNN uses three as the number of neighbors.

The distributions of the absolute error and relative error for the XEQ, WKS, and SH stations are shown in Fig. 14. The prediction accuracy indexes are shown in Tables 7–9.

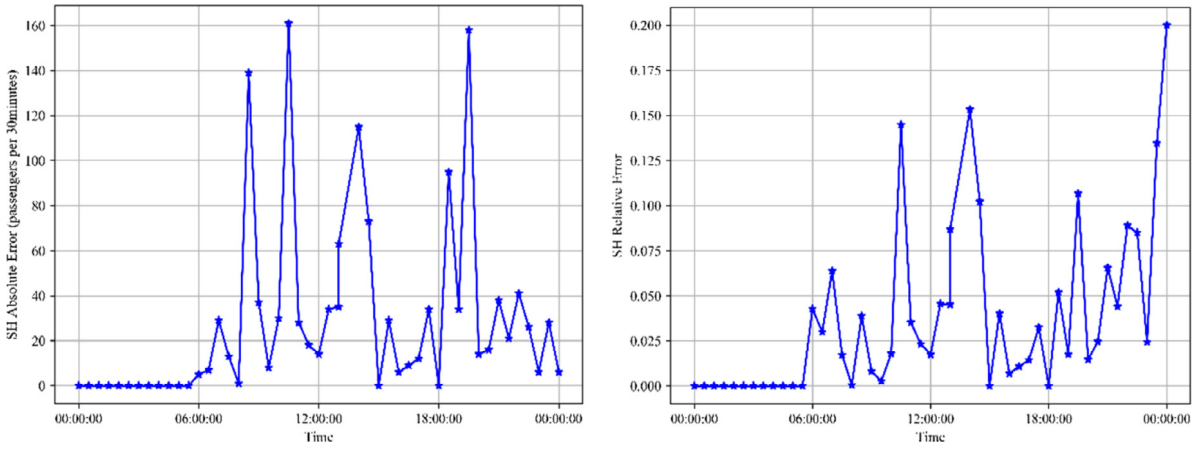

Fig. 12. RBF absolute error and relative error for the SH station.

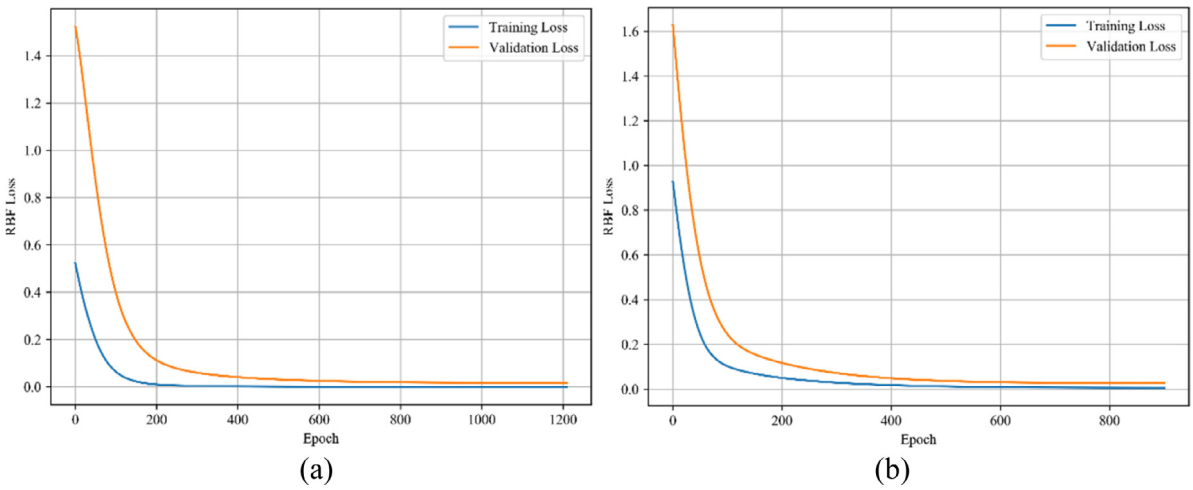

Fig. 13. Training loss and validation loss of the (a) XEQ station and (b) WKS station during the 08:30–09:00 period.

Table 9
The RMSE values of the XEQ, WKS, and SH stations.

RMSE	BP	Wavelet-SVM	KNN	RBF
XEQ	98.5032	72.5410	43.3857	21.1225
WKS	131.6676	114.5748	121.0723	112.9729
SH	74.5632	60.2901	58.4507	54.9641

Fig. 14 shows that the dynamic RBF has the smallest absolute error and relative error among the four methods. Because the model input terms are dynamically determined based on the train timetable, the arrival station can be precisely determined for trains at any time. Because passenger flow control data are adopted, the passenger flow features are accurately captured. Therefore, the dynamic RBF outperforms the BP neural network, Wavelet-SVM and KNN models in predicting the outbound volume of the XEQ, WKS, and SH stations.

Tables 7–9 show the MAPE, VAPE, and RMSE of the XEQ, WKS, and SH stations using the four methods. The smaller dynamic RBF values indicate a higher accuracy than those of the BP neural network, Wavelet-SVM methods and the KNN model. In addition, a large passenger flow during peak hours under passenger flow control was predicted for the XEQ station, as shown in Fig. 14. The proposed dynamic RBF outperforms the BP neural network, the Wavelet-SVM and the KNN model for the XEQ station case, especially in scenarios involving large passenger flows. In the predictions for both the WKS and SH stations, the dynamic RBF model outperforms the BP neural network, Wavelet-SVM and the KNN models.

The dynamic RBF method achieves better performances than do the BP neural network, Wavelet-SVM and the KNN model not only in normal passenger flow scenarios but also for passenger flow under passenger control. Taking passenger flow control measures in advance can alleviate congestion in metro stations. In addition, the dynamic RBF can be used to verify the validity of implemented passenger flow control measures. Metro stations with passenger flow control in effect (with the exception of the target station) can be pinpointed.

5. Conclusions

To address passenger flow prediction under passenger flow control, this paper proposes an RBF neural network to predict the outbound volumes of stations using the train timetable, passenger flow, and passenger flow control data. One disadvantage of RBF is that the initial model may include a large number of candidate terms. To address this problem, the initial model inputs are selected by limiting the running time from relative stations to the target station to a specified duration using the train timetable to avoid overfitting. Next, the GCV and ERR criteria are adopted to filter the model inputs. Passenger flow control in the Beijing metro is utilized to adjust the model and improve the prediction accuracy. Then, a layer of dynamic input to the RBF is constructed. Another disadvantage of RBF is that the center of the radial basis function and the number of neurons in the hidden layer are difficult to determine. To overcome this problem, we used FCM clustering and the OLS algorithm to determine the centers and weights for our dynamic RBF. The number of neurons in the hidden layer is determined by the number of cluster centers in FCM, and the optimal number of clusters is selected by the minimum absolute error.

We tested the proposed RBF model on three representative scenarios and compared its result with those of the BP neural network, the Wavelet-SVM and the KNN models to examine the prediction accuracy. First, the average MAPE, VAPE, and RMSE of our predictions are 4.5441, 0.3144, and 63.0198, respectively, showing that the proposed model has excellent accuracy for the XEQ, WKS, and SH station predictions. Second, the results show that the proposed model outperforms the BP neural network, the Wavelet-SVM and the KNN model. Specifically, the average RMSE decreased by 37.9592%, 26.6422% and 15.4321% and the average MAPE decreased by 23.5833%, 20.0855% and 21.8502% when comparing the model results to the BP neural network, the Wavelet-SVM and the KNN model, respectively. Third, the proposed model performs particularly well in large passenger flow scenarios because the passenger flow factor of the most relevant station can be selected by including a consideration of passenger flow control in the relative stations. Meanwhile, the dynamic optimal numbers of clusters based on the minimum absolute error determines the number of neurons of the RBF layer dynamically to improve the prediction accuracy. The results provide insights about which stations have the strongest impacts on the target station, which enables us to determine where further passenger flow control policy should be applied to limit the outbound volume of the target station to minimize safety concerns during peak hours. However, our RBF model also has some limitations, for example, it has a relatively complex hidden layer and a lengthy computational time.

This study predicts passenger flow only in scenarios that include passenger flow control, large passenger flow volume, and normal passenger flow. In future studies, we plan to predict passenger flows of all stations and consider more complex setups

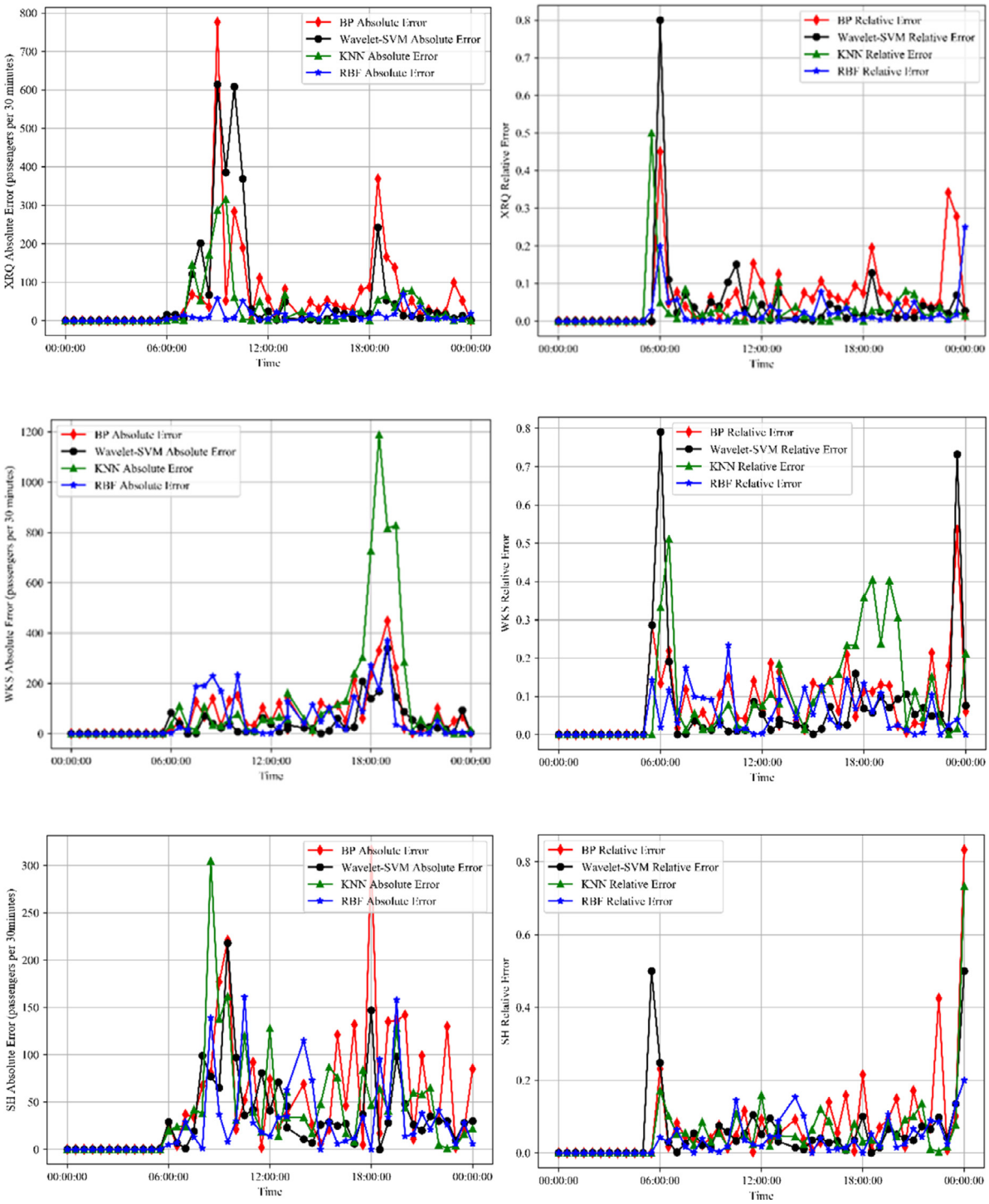

Fig. 14. Absolute and relative prediction errors of the XEQ, WKS and SH stations.

in an entire network 30 min in advance. In addition, we will explore a better way to determine the center of the RBF neural network in future studies.

Acknowledgments

This work is financially supported by the National Natural Science Foundation of China (No. 71601018 and 71871012). The authors acknowledge with gratitude the suggestions and assistance of Jacci Ziebert and anonymous referees who helped to improve the presentation of this paper.

Declaration of competing interest

No author associated with this paper has disclosed any potential or pertinent conflicts which may be perceived to have impending conflict with this work. For full disclosure statements refer to https://doi.org/10.1016/j.asoc.2019.105620.

References

[1] H. Jiang, D.M. Levinson, Accessibility and the evaluation of investments on the Beijing subway, J. Transp. Land Use. 10 (2016) http://dx.doi.org/10.5198/jtlu.2016.884.

[2] M. Ni, Q. He, J. Gao, Forecasting the subway passenger flow under event occurrences with social media, IEEE Trans. Intell. Transp. Syst. 18 (2017) 1623–1632, http://dx.doi.org/10.1109/TITS.2016.2611644.
[3] S.Z. Zhao, T.H. Ni, Y. Wang, X.T. Gao, A new approach to the prediction of passenger flow in a transit system, Comput. Math. Appl. 61 (2011) 1968–1974, http://dx.doi.org/10.1016/j.camwa.2010.08.023.
[4] X. Xu, H. Li, J. Liu, B. Ran, L. Qin, Passenger flow control with multi-station coordination in subway networks: Algorithm development and real-world case study, Transp. B. 7 (1) (2019) 446–472, http://dx.doi.org/10.1080/21680566.2018.1434020.
[5] X. Xu, J. Liu, H. Li, J. Hu, Analysis of subway station capacity with the use of queueing theory, Transp. Res. C 38 (2014) 28–43.
[6] X. Xu, L. Xie, H. Li, L. Qin, Learning the route choice behavior of subway passengers from AFC data, Expert Syst. Appl. 95 (2018) 324–332.
[7] G. Xiao, Z. Juan, C. Zhang, Detecting trip purposes from smartphone-based travel surveys with artificial neural networks and particle swarm optimization, Transp. Res. C 71 (2016) 447–463, http://dx.doi.org/10.1016/j.trc.2016.08.008.
[8] H. Trenchard, M. Perc, Energy saving mechanisms collective behavior and the variation range hypothesis in biological systems: A review, BioSystems 147 (2016) 40–66, http://dx.doi.org/10.1016/j.biosystems.2016.05.010.
[9] D. Helbing, D. Brockmann, T. Chadefaux, K. Donnay, U. Blanke, O. Woolley-Meza, M. Moussaid, A. Johansson, J. Krause, S. Schutte, M. Perc, Saving Human Lives: What Complexity Science and Information Systems Can Contribute, 2014, http://dx.doi.org/10.1007/s10955-014-1024-9.
[10] X. Xu, J. Liu, H. Li, M. Jiang, Capacity-oriented passenger flow control under uncertain demand: Algorithm development and real-world case study, Transp. Res. Part E Logist. Transp. Rev. 87 (2016) 130–148, http://dx.doi.org/10.1016/j.tre.2016.01.004.
[11] A. Bezuglov, G. Comert, Short-term freeway traffic parameter prediction: Application of grey system theory models, Expert Syst. Appl. 62 (2016) 284–292, http://dx.doi.org/10.1016/j.eswa.2016.06.032.
[12] D. Pavlyuk, Short-term traffic forecasting using multivariate autoregressive models, in: Procedia Eng., Elsevier B.V., 2017, pp. 57–66, http://dx.doi.org/10.1016/j.proeng.2017.01.062.
[13] Y. Sun, B. Leng, W. Guan, A novel wavelet-SVM short-time passenger flow prediction in Beijing subway system, Neurocomputing 166 (2015) 109–121, http://dx.doi.org/10.1016/j.neucom.2015.03.085.
[14] Y. Wei, M.-C. Chen, Forecasting the short-term metro passenger flow with empirical mode decomposition and neural networks, Transp. Res. C 21 (2012) 148–162.
[15] Y. Li, X. Wang, S. Sun, X. Ma, G. Lu, Forecasting short-term subway passenger flow under special events scenarios using multiscale radial basis function networks, Transp. Res. C 77 (2017) 306–328, http://dx.doi.org/10.1016/j.trc.2017.02.005.
[16] X. Ma, Z. Tao, Y. Wang, H. Yu, Y. Wang, Long short-term memory neural network for traffic speed prediction using remote microwave sensor data, Transp. Res. C 54 (2015) 187–197, http://dx.doi.org/10.1016/j.trc.2015.03.014.
[17] L. Liu, R.-C. Chen, A novel passenger flow prediction model using deep learning methods, Transp. Res. C 84 (2017) 74–91, http://dx.doi.org/10.1016/j.trc.2017.08.001.
[18] J. Roos, G. Gavin, S. Bonnevay, A dynamic Bayesian network approach to forecast short-term urban rail passenger flows with incomplete data, Transp. Res. Procedia 26 (2017) 53–61, http://dx.doi.org/10.1016/j.trpro.2017.07.008.
[19] U. Ryu, J. Wang, T. Kim, S. Kwak, J. U, Construction of traffic state vector using mutual information for short-term traffic flow prediction, Transp. Res. C 96 (2018) 55–71, https://doi.org/10.1016/j.trc.2018.09.015.
[20] L. Qu, W. Li, W. Li, D. Ma, Y. Wang, Daily long-term traffic flow forecasting based on a deep neural network, Expert Syst. Appl. 121 (2019) 304–312, http://dx.doi.org/10.1016/j.eswa.2018.12.031.
[21] H. Tan, L. Qin, Z. Jiang, Y. Wu, B. Ran, A hybrid deep learning based traffic flow prediction method and its understanding, Transp. Res. C 90 (2018) 166–180, http://dx.doi.org/10.1016/j.trc.2018.03.001.
[22] Y.W. Linchao Li, Lingqiao Qin, Xu Qu, Jian Zhang, B. Ran, Day-ahead traffic flow forecasting based on a deep belief network optimized by the multi-objective particle swarm algorithm, Knowledge-Based Syst. (2019) http://dx.doi.org/10.1016/j.knosys.2019.01.015.
[23] J. Xiao, Z. Xiao, D. Wang, J. Bai, V. Havyarimana, F. Zeng, Short-term traffic volume prediction by ensemble learning in concept drifting environments, Knowl.-Based Syst. 164 (2019) 213–225, http://dx.doi.org/10.1016/j.knosys.2018.10.037.
[24] D. Wei, Network traffic prediction based on RBF neural network optimized by improved gravitation search algorithm, Neural Comput. Appl. 28 (2017) 2303–2312, http://dx.doi.org/10.1007/s00521-016-2193-z.
[25] W. Yu, L. Liu, W. Zhang, Traffic prediction method based on RBF neural network with improved artificial bee colony algorithm, in: Proc. - 8th Int. Conf. Intell. Networks Intell. Syst. ICINIS 2015, 2016, pp. 141–144, http://dx.doi.org/10.1109/ICINIS.2015.19.
[26] P. Wang, C. Wu, X. Gao, Research on subway passenger flow combination prediction model based on RBF neural networks and LSSVM, in: Proc. 28th Chinese Control Decis. Conf. CCDC 2016, 2016, pp. 6064–6068, http://dx.doi.org/10.1109/CCDC.2016.7532085.
[27] D. Chen, Research on traffic flow prediction in the big data environment based on the improved RBF neural network, IEEE Trans. Ind. Inform. 13 (2017) 2000–2008, http://dx.doi.org/10.1109/TII.2017.2682855.
[28] X. Jiang, L. Zhang, M.X. Chen, Short-term forecasting of high-speed rail demand: A hybrid approach combining ensemble empirical mode decomposition and gray support vector machine with real-world applications in China, Transp. Res. C 44 (2014) 110–127, http://dx.doi.org/10.1016/j.trc.2014.03.016.
[29] S.A. Billings, H.L. Wei, M.A. Balikhin, Generalized multiscale radial basis function networks, Neural Netw. 20 (2007) 1081–1094, http://dx.doi.org/10.1016/j.neunet.2007.09.017.
[30] H. De Leon-delgado, R.J. Praga-alejo, D.S. Gonzalez-gonzalez, M. Cantú-sifuentes, Multivariate statistical inference in a radial basis function neural network, Expert Syst. Appl. 93 (2018) 313–321.
[31] J. Alam, M. Hassan, A. Khan, A. Chaudhry, Robust fuzzy RBF network based image segmentation and intelligent decision making system for carotid artery ultrasound images, Neurocomputing 151 (2015) 745–755.
[32] W. Jia, D. Zhao, L. Ding, An optimized RBF neural network algorithm based on partial least squares and genetic algorithm for classification of small sample, Appl. Soft Comput. J. 48 (2016) 373–384, http://dx.doi.org/10.1016/j.asoc.2016.07.037.
[33] S.A. Billings, H.L. Wei, The wavelet-NARMAX representation: A hybrid model structure combining polynomial models with multiresolution wavelet decompositions, Internat. J. Systems Sci. 36 (2005) 137–152, http://dx.doi.org/10.1080/00207720512331338120.
[34] H.L. Wei, S.A. Billings, J. Liu, Term and variable selection for non-linear system identification, Int. J. Control 77 (2004) 86–110.
[35] Y. Duan, Y. Lv, Y.L. Liu, F.Y. Wang, An efficient realization of deep learning for traffic data imputation, Transp. Res. C 72 (2016) 168–181.
[36] P.P. Balestrassi, E. Popova, A.P. Paiva, J.W. Marangon Lima, Design of experiments on neural network's training for nonlinear time series forecasting, Neurocomputing 72 (2009) 1160–1178, http://dx.doi.org/10.1016/j.neucom.2008.02.002.
[37] F. Toque, E. Come, M.K. El Mahrsi, L. Oukhellou, Forecasting dynamic public transport origin-destination matrices with long-short term memory recurrent neural networks, in: 2016 IEEE 19th Int. Conf. Intell. Transp. Syst, IEEE, 2016, pp. 1071–1076.